Vol 18 No 5, May 2009
1674-1056/2009/18(05)/2016-08
Chinese Physics B
© 2009 Chin. Phys. Soc.
and IOP Publishing Ltd

Controlled growth and field emission of vertically aligned AlN nanostructures with different morphologies*

Liu Fei(刘 飞)†, Su Zan-Jia(苏赞加), Liang Wei-Jie(梁炜杰),
Mo Fu-Yao(莫富尧), Li Li(李 力), Deng Shao-Zhi(邓少芝),
Chen Jun(陈 军), and Xu Ning-Sheng(许宁生)

Guangdong Province Key Laboratory of Display Material and Technology, School of Physics and Engineering, Sun Yat-sen University, Guangzhou 510275, *China*

(Received 13 February 2009; revised manuscript received 23 February 2009)

The controllable growth of three different morphologies of AlN nanostructures (nanorod, nanotip and nanocrater) arrays are successfully realized by using chemical vapour deposition (CVD) technology. All three nanostructures are of single crystal h-AlN with a growth orientation of [001]. Their growth is attributed to the vapour-liquid-solid (VLS) mechanism. To investigate the factors affecting field emission (FE) properties of AlN nanostructures, we compare their FE behaviours in several aspects. Experimental results show that AlN nanocrater arrays possess the best FE properties, such as a threshold field of 7.2 V/μm and an emission current fluctuation lower than 4%. Moreover, the three AlN nanostructures all have good field emission properties compared with a number of other excellent cathode nanomaterials, which suggests that they are future promising FE nanomaterials.

Keywords: AlN, field emission (FE), vapour-liquid-solid (VLS), chemical vapour deposition (CVD)
PACC: 7280E, 7970, 6810, 8115H

1. Introduction

Nanomaterials have aroused the interest of many researchers since the carbon nanotube was first found by Iijima.[1] There have now emerged many nanostructures that were considered as potential field emission (FE) materials because of their larger aspect ratios than bulk materials, such as carbon nanotubes,[2,3] boron nanomaterials[4−6] and CuO nanomaterials.[7,8] But when the excellent field emission behaviours of diamond film were first demonstrated by Geis,[9] wide bandgap conductors were expected to have a more promising prospect in the FE area than most other materials because they possess negative or a little positive electron affinity,[10,11] which can make electrons in the conduction band escape into the vacuum more easily. As one of the most important wide bandgap nanomaterials, aluminium nitride has been investigated extensively due to its high melting point ($> 2300\,^{\circ}$C), high thermal conductivity ($K \approx 320$ W/(m·k)), large exciton binding energy and strong endurance to harsh environments.[12−15] Although various methods have been developed to prepare AlN nanostructures with different morphologies, such as nanotips,[16−18] nanorods,[19,20] nanowires,[21,22] and nanobelts,[23] only a little attention[16−18,21] has been paid to research on their field emission properties. In addition, to our knowledge, what determines the field emission behaviours of AlN nanostructures is still unknown until now, which has restricted their practical applications in the field emission area.

We report on the controlled growth of single-crystal AlN nanorod, nanotip and nanocrater vertical arrays on a large scale by using chemical vapour deposition (CVD) technology. In addition, they are characterized by using a scanning electron microscope

*Project supported by the National Basic Research Program of China (Grant No 2007CB935500), the National High Technology Research and Development Program of China (Grant No 2007AA03Z305), the National Science Foundation for Young Scientists of China (Grant No 50802117), the National Joint Science Fund with Guangdong Province (Grant Nos U0634002 and U0734003), the Specialized Research fund for the Doctoral Program of High Education of China (Grant No 20070558063), the Science and Technology Department of Guangdong Province, the Education Department of Guangdong Province, and the Science and Technology Department of Guangzhou City, China.
†Corresponding author. E-mail: liufei@mail.sysu.edu.cn

(SEM) and transmission electron microscope (TEM) in order to analyse their morphological and structural features. Moreover, their field emission properties are compared with each other to understand what effects both the morphologies and the growth densities of the AlN nanostructures will have on their field emission behaviours. The possible growth mechanisms and the field emission mechanisms of three different morphologies of AlN nanostructures are also discussed here.

2. Experiment

2.1. Synthesis of AlN nanostructures with different morphologies

In this experiment, the CVD method was used to synthesize AlN nanostructures, and the scheme of the tube furnace system is shown in Fig.1. Al powders (chemical purity 99.99%) were used as source materials and loaded in an alumina boat. Fe_3O_4 nanoparticles with diameters less than 10 nm were synthesized through high temperature solution phase reaction[24,25] and spread over the silicon substrate as catalysts. A two-step increasing temperature method was used to synthesize AlN nanostructures. The first step was that when the temperature of the central region of the furnace reached 400 °C, the reaction vessel was maintained for 20–30 min. The base pressure of the chamber was better than 5 Pa and the flow rate of N_2 was kept at 200 sccm. The second step was that when the temperature of the reaction region was raised to 750–1000 °C, the carrier gas of mixed N_2 and NH_3 was fed into the chamber rapidly. The flow rate ratio of N_2 to NH_3 was kept at 200:5–200:20 sccm and the reaction pressure was maintained at 1×10^4 Pa. The reaction lasted 1–2 h, and the alumina boat was placed in the central region through the process. By controlling the experimental conditions, single-crystal AlN nanostructures with different morphologies were successfully fabricated. Their detailed growth conditions are listed in Table 1.

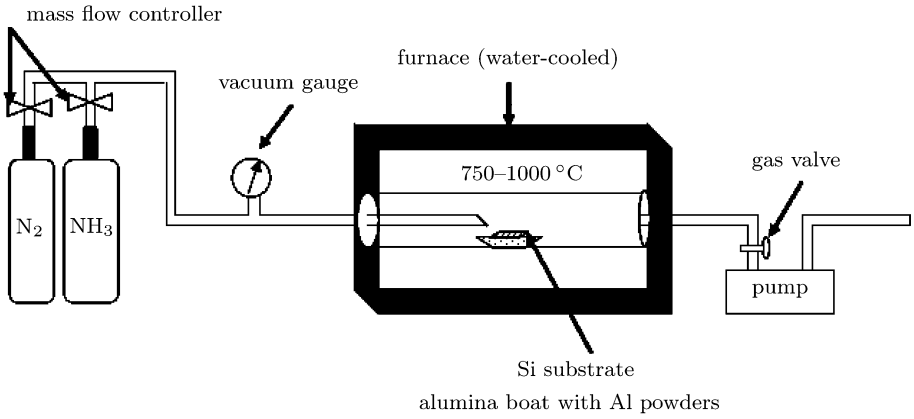


Fig.1. Scheme of the chemical vapour deposition system in this experiment.

Table 1. Growth conditions for different morphologies of AlN nanostructures.

morphology	growth conditions				
	source materials	the gas ratio of N_2 to NH_3/sccm	reaction pressure/Pa	growth temperature/°C	synthesis time/h
Nanocone	Al powders	200 : 10	5×10^4	800	2
Nanorod	Al powders	200 : 10	5×10^4	1000	2
Nanocrater	Al powders	200 : 10	5×10^4	900	2

2.2. Characterization of AlN nanostructures with different morphologies

A field-emission type scanning electron microscope (XL-SFEG SEM, FEI Corp.) was used to investigate the morphological features of AlN nanostructures. A TEM (Tecnai-20 TEM, PHILIPS) and selected area electron

diffraction (SAED) were employed to characterize their crystalline structures. The field emission properties of AlN nanostructures with different morphologies were investigated on the field emission analysis system.

3. Results and discussion

Three morphologies of AlN nanostructure (nanocone, nanorod and nanocrater) arrays were obtained on silicon substrates by changing reaction conditions. Figure 2 shows their corresponding SEM images, revealing their detailed morphological features. From Fig.2(a), the AlN nanocones are observed to have sharp tips and

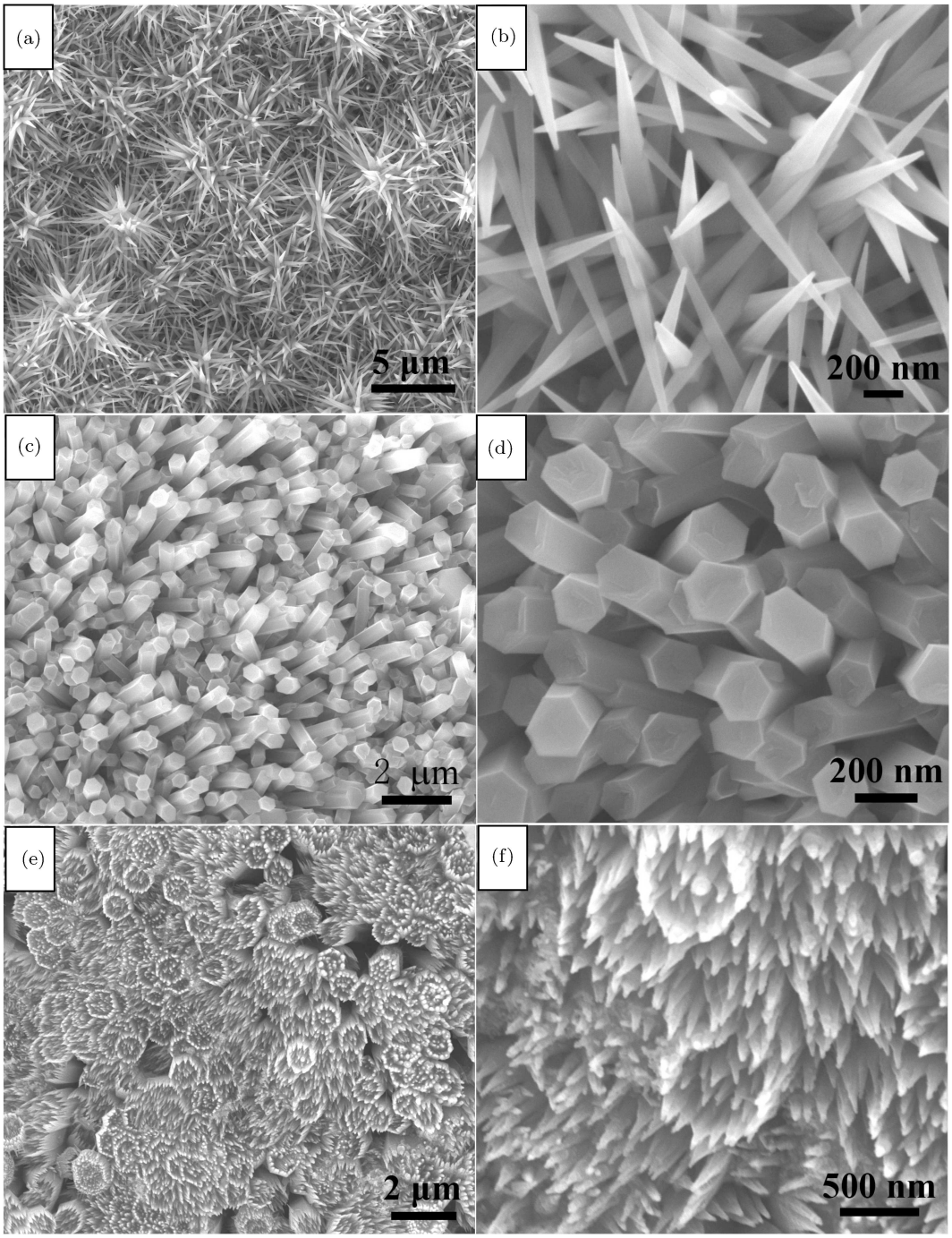


Fig.2. SEM images of AlN nanostructures, where panels (a) and (b) show low-resolution and high-resolution SEM images of the AlN nanocones, panels (c) and (d) indicate typical SEM images of the AlN nanorods in low magnification and high magnification, and panels (e) and (f) refer to the low magnification and high magnification images of the AlN nanocraters, respectively.

stand vertically on the substrate surface. The high resolution SEM image of AlN nanocones is shown in Fig.2(b). It is seen that these nanocones have a length of about 2 μm and a mean radius of 40 nm as well as they have a smooth surface and high growth density. Figure 2(c) shows the SEM image of AlN nanorod arrays on a large scale. It is observed that these nanorods are perpendicular to the substrate surface and well-aligned. From the high magnification SEM image in Fig.2(d), these nanorods are found to have well-faceted hexagonal shapes and the same diameters throughout the nanostructure. These nanorods are about 2 μm in length and about 150 nm in diameter. The SEM image of large area AlN nanocrater arrays is shown in Fig.2(e). One can see that these AlN nanostructures grow in the direction perpendicular to the silicon substrate surface and have uniform shapes. The nanostructures are composed of many surrounding AlN nanocones with similar aspect ratios and have crater-like shapes, which is the reason why they are referred to as nanocraters. Their outer diameters range from 400 to 500 nm and their average length is 2 μm. The aspect ratios of these three AlN nanostructures are 50, 23 and 10, respectively as listed in Table 2.

Table 2. Morphological and field emission parameters for as-prepared AlN nanostructures.

	FE properties					
morphology	aspect ratio	turn on field at 10 μA/(V/μm)	threshold field at 1 mA/(V/μm)	nanostructure density/cm^{-2}	β	emission instability in 2 hours
nanocone	50	4.2	11.3	2.2×10^9	1740	9 %
nanorod	23	4.9	12.4	1.5×10^9	1250	7 %
nanocrater	10	3.9	7.2	3×10^8	2140	4 %

In order to confirm the detailed crystalline structures of these three AlN nanostructures, their corresponding individual nanostructure was investigated by using the TEM technique. A typical TEM image of an AlN nanocone is shown in Fig.3(a), from which one can see that the diameters of the nanocones gradually decrease from the bottom to the top. The corresponding selected area electron diffraction (SAED) patterns are given in Fig.3(b). By identifying their clear diffraction spots, it is suggested that these nanocones each have a perfect single crystalline h-AlN structure and have a growth direction of [001]. Also, the AlN nanorods have a uniform diameter over the whole length as shown Fig.3(c). Further SAED characterization shown in Fig.3(d) indicates that the AlN nanorods are also of h-AlN single crystalline structure and grow along the [001] direction, which is the same as the nanocones. Figure 3(e) shows the general TEM image of AlN nanocraters. It is seen that the nanocrater is composed of several surrounding nanocones, which is consistent with what the SEM image of Fig.2(f) shows. The SAED technique was used to investigate each nanocone in the nanocrater, and a typical SAED pattern of a nanocone (white ellipse) is indicated in Fig.3(f). It is noted that nanocones appear to have the same diffraction spots, which proves that their growth axes are all along the [001] direction. So a conclusion can be drawn that no matter what morphology these AlN nanostructures belong to, they are all single crystals with a growth orientation of [001].

According to the observations reported above, we prefer to use the vapour-liquid-solid (VLS) mechanism to explain the formation of AlN nanostructures. From these TEM images, we do not find any catalyst existing at the top of these three nanostructures though the Fe_3O_4 nanoparticles are used as catalyst. So it is proposed that the growth model of these nanostructures is the bottom growth model because the tight bonding force may exist between the catalyst and the substrate at the beginning of the growth as explained in Ref.[26]. The mechanism of forming different morphologies of AlN nanostructures may be the diffusion mediated growth mechanism.[20] According to this mechanism, AlN precursors have different diffuse lengths for different growth planes, and these growth planes should have different growth rates at different temperatures at the same time. The anisotropy of the growth plane at different temperatures will induce the formation of nanorod or nanocone, i.e. high temperature is more beneficial to the synthesis of AlN nanorods. When the growth temperature is slightly increased (still lower than the temperature of the nanorod) at the molecular ratio of the reaction gas (NH_3/N_2) of the nanocone, AlN nanocraters can be synthesized. Under this condition, more AlN vapours can dissolve in the catalyst

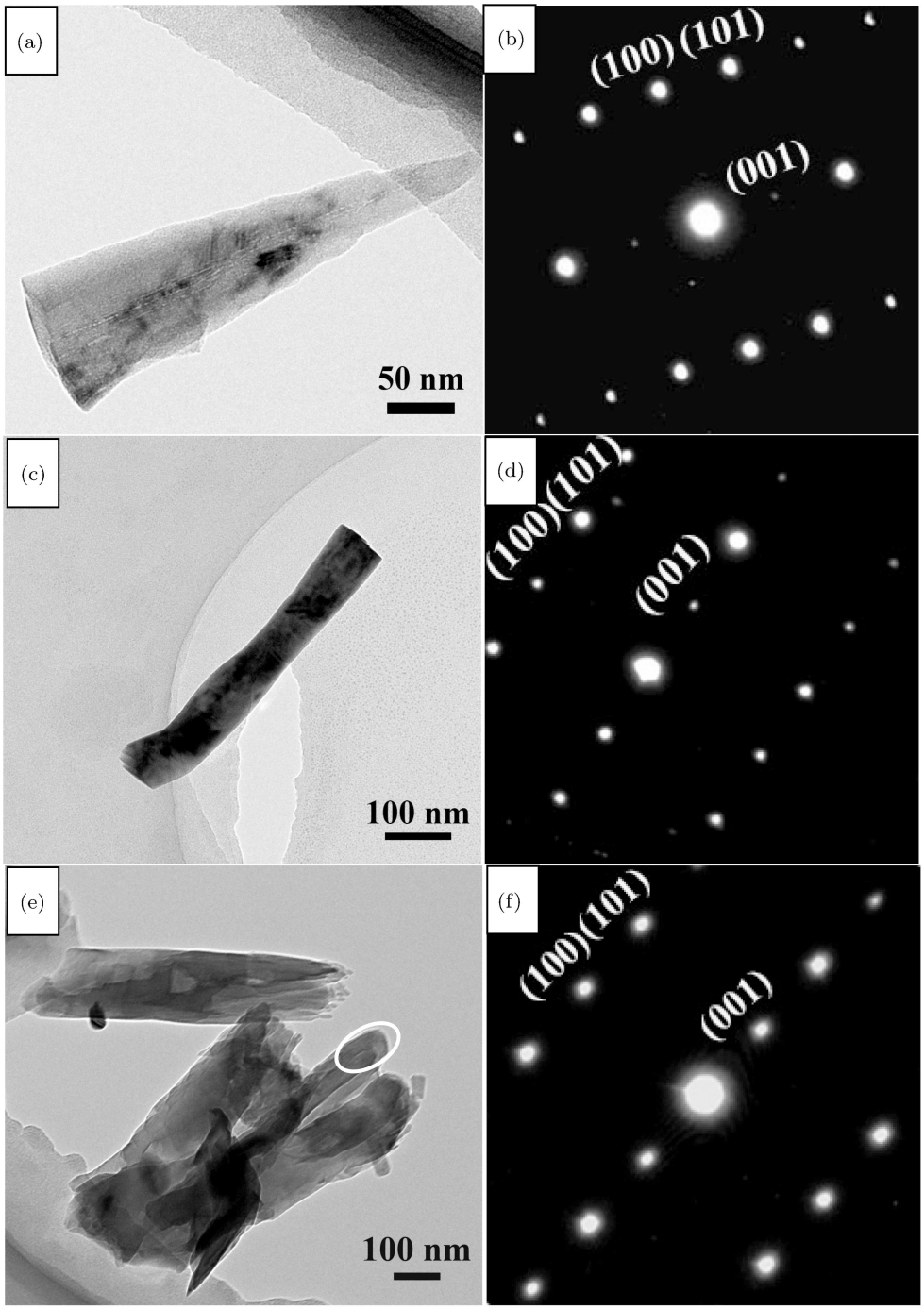


Fig.3. Typical TEM images and SAED patterns of three kinds of AlN nanostructures: AlN nanocones ((a) and (b)), AlN nanorods ((c) and (d)), and AlN nanocraters ((e) and (f)) with the SAED pattern in Fig.3(f) corresponding to the white ellipse region in Fig.3(e).

solution in the growth stage than in the formation stage of AlN nanocones. Subsequently more AlN seeds can be separated from oversaturated solutions because of the overmuch supplement of the vapours in the following stage. Because the concentration of the catalyst is too large, the density of the catalyst becomes very high and the distance between the catalysts turns short accordingly. Driven by high temperature, the neighbour catalysts migrate to gather together, thus forming larger precursors for the new seeds in synthesizing new nanostructures, which should be the most stable structures from the viewpoint of energy. Finally, the nanocraters are fabricated from these gathered precursors as the progress of the reaction goes on.

Steric overcrowding[27−29] is thought of as the possible aligned mechanism of AlN nanostructure arrays. It is suggested that the temperature is a key factor in determining the morphologies of AlN nanostructures. There also exist some other growth parameters affecting the growth of the AlN nanostructures. The AlN nanostructures can be obtained only if the flow rate ratio of N_2 to $NH_3$is in some range. When the flow rate ratio of N_2 to NH_3 is adjusted to be lower than 200:5, no AlN nanostructure can be synthesized. When the ratio is adjusted to higher than 200:40, only AlN nanoparticle thin film can be fabricated. The growth pressure also has some influence on their morphology. If the growth pressure is lower than 10^3 Pa, only AlN nanoparticles can be found on the substrate. Meanwhile, the reaction pressure and the flow ratio of the mixed gas can also affect the growth density of the AlN nanostructures, and their optimal growth conditions for AlN nanostructures are found to be 5×10^4 Pa and 200:10 in our experiments, respectively. More detailed growth parameters are provided in Table 1.

To investigate the possibility for the AlN nanostructures to be used as cold cathode nanomaterials, their field emission measurement is carried out in the field emission analysis system, whose base pressure is lower than 3×10^{-7} Pa. The field current density (J)-electric field (E) curves, i.e. J–E curves, and Fowler–Nordheim (FN) plots of the nanocones, the nanorods and the nanocraters are shown in Fig.4(a) and 4(b), respectively. By comparing their FE behaviours, it is clear that the AlN nanocraters have the best FE performance with a turn-on field (10 μA/cm^2) of 3.9 V/μm and a threshold field (1 mA/cm^2) of 7.2 V/μm. It is also seen that the FE properties of the AlN nanocones are better, and those of the AlN nanorods are the worst among them as summarized in Table 2. But for the AlN nanorods with the worst FE performance, their FE behaviours are still better than those of most of FE nanomaterials, such as ZnO, WO_3 and CuO, which suggests that AlN nanostructures are one of the most promising FE materials in the future. In addition, their FN plots are observed to be almost linear, which conforms to the classical FN theory well.[30] The values of enhancement factor β for the AlN nanostructures are also listed in Table 2, which reflect the amplification ability of macroscopic field. Their values are easily obtained by calculating the slopes of the FN curves. Obviously, of these three nanostructures the nanocrater arrays have the largest value of β (2140) while the nanorod arrays have the smallest value of β (1250).

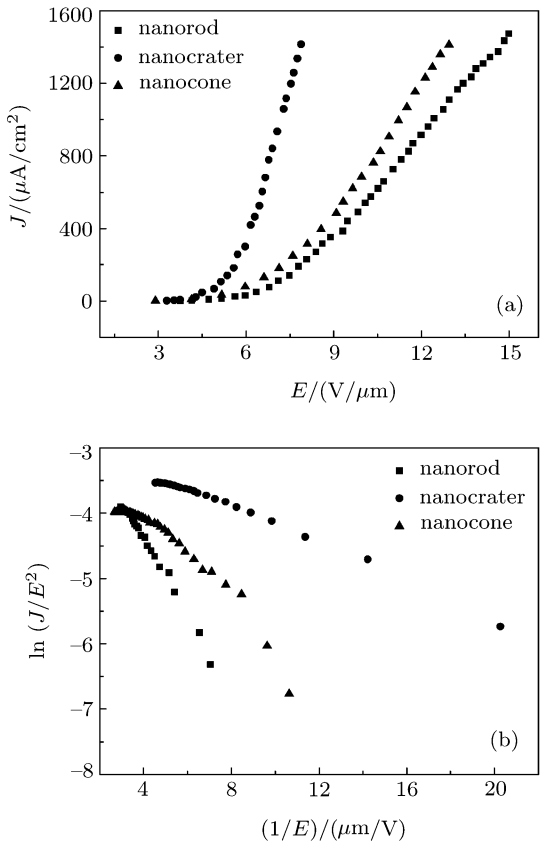


Fig.4. Field current density–electric field (J–E) curves for AlN nanostructures with different morphologies (a) and their corresponding FN plots (b).

How the morphologies of AlN nanostructures have an effect on their FE properties is an important point, which is related to their application in the field emission area. We propose the following interpretations to analyse the possible FE mechanism, which leads to their different FE performances. According to the metal-insulator-vacuum (MIV) theory,[31] the microscopic field $E_{\rm M}$ acting on the tip of nanoscale protrusion is proportional to enhancement factor β, which is given by

$$E_{\rm M} = \beta E = \beta \frac{V}{d}, \tag{1}$$

where V is the applied voltage across the anode and the cathode, and E is the applied macroscopic field. The enhancement factor β can be expressed as[32]

$$\beta = \frac{\left(\lambda^2-1\right)^{1.5}}{\lambda \ln\left[\lambda + \left(\lambda^2-1\right)^{1/2}\right] - \left(\lambda^2-1\right)^{1/2}}, \tag{2}$$

where $\lambda = l/r$ is the aspect ratio i.e. the ratio between the length of the nanostructure and its top radius. As discussed in the above theory, the higher β value of

the nanocones ensures that they have stronger ability to amplify macroscopic field than the nanorods under the same applied field, which makes tunnel emission easier. As a result, the nanocones should possess better field emission behaviours than nanorods, for they have an aspect ratio of about 50 larger than that of nanorods (23) as well as a similar growth density to that of nanorods (about $2\times10^9/\mathrm{cm}^2$), which accords with our FE measurement results well in Table 2.

As for the AlN nanocraters having the best FE behaviours among them, the field screen effect[33,34] must be considered in their field emission process. It is known that if the growth density of the nanostructure is very high, the surface of the nanostructured film will be very close to a plane, which will prevent the macroscopic electrical field from penetrating into the nanostructures film,[33] thereby reducing the local field amplification existing among the nanostructures and increasing the difficulty in operating the electron emission. Nanocone array and nanocrater array both consist of many nanocones with similar aspect ratios, and their only difference is that their growth densities are different. It is obvious that the field enhancement function of nanocraters is more prominent because their growth density ($3\times10^8/\mathrm{cm}^2$) is more suitable than that of nanocones ($2.2\times10^9/\mathrm{cm}^2$) for emission based on the field screen effect theory.[33,34] Because the good alignment of the nanostructures is favourable for their FE properties, the effect of the alignment of AlN nanostructures on their FE properties should also be considered here. As is well known, the aligned nanostructures can ensure less mutual influence existing among the microscopic field of the nanostructures than the random-arranged nanostructures, thus weakening the effect of the screen effect from the nanostructures and increasing the possibility of emission operation. Considering that the nanocraters have a better alignment than nanocones or nanorods as well as possessing the most suitable growth density, they should have the most excellent FE performance, which accords with our observations. Moreover, it is proposed that the morphology, the growth density and the alignment of the AlN nanostructures determine their FE behaviours to a great extent.

The emission stability is another important point for AlN nanostructures, which should attract our attention. The stability curves of these three AlN nanostructures are given in Fig.5. Because the appearance of instability at high working currents is more important than at low currents in the sense of application, the emission current was kept at 1080 μA no matter whether they are nanocones or nanorods or nanocraters during our measurement. The whole measurement lasted 2 h. Through the comparison among three morphologies of AlN nanostructures, the nanocraters are found to possess the stablest emission performance with a current fluctuation lower than 4% as indicated in Table 2. Both AlN nanorods and nanocones also exhibit stable field emission behaviours, and their current fluctuations are lower than 7% and 9%, which is good enough for the potential application in field emission area. Considering all the field emission behaviours of these three AlN nanostructures, we can draw a conclusion that the AlN nanocrater arrays have the best FE performance, which should have the most promising prospect in FE applications.

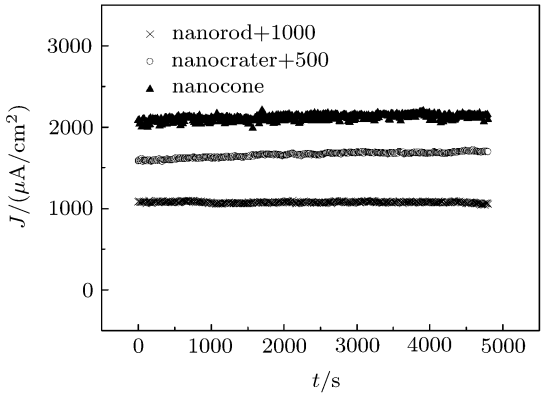


Fig.5. Stability curves for AlN nanostructures with different morphologies in the field emission process.

4. Conclusions

Aligned AlN nanostructure (nanocones, nanorods and nanocraters) arrays are fabricated in a large area under control. Their structures are all single crystal wurtzite structures with a length of several micrometres. A detailed comparison among the FE behaviours of these AlN nanostructures shows that the AlN nanocrater arrays exhibit the best FE behaviours among them in the sense of emission operation and stability, and that the morphology, the growth density and the alignment of the nanostructures play a very important role in determining their FE properties. Moreover, the three morphologies of AlN nanostructures all have good field emission behaviours, such as stable emission and lower threshold field, which suggests that they possibly will be ideal cathode nanomaterials in the future.

Acknowledgement

We are grateful to the Electron Microscopy Centre in Sun Yat-Sen University for SEM and TEM characterizations.

References

[1] Iijima S 1991 *Nature* **354** 56
[2] Choi W B 1999 *Appl. Phys. Lett.* **75** 3129
[3] Ma W C, Wang E G, Zhou W Z, Jefferson D A, Chen J, Deng S Z, Xu N S and Yuan J 1999 *Appl. Phys. Lett.* **75** 3105
[4] Bao L H, Li C, Tian Y, Tian J F, Hui C, Wang X J, Shen C M and Gao H J 2008 *Chin. Phys.* B **17** 4247
[5] Wang X J, Tian J F, Bao L H, Yang T Z, Hui C, Liu F, Shen C M, Xu N S and Gao H J 2008 *Chin. Phys.* B **17** 3827
[6] Bao L H, Li C, Tian Y, Tian J F, Hui C, Wang X J, Shen C M and Gao H J 2008 *Chin. Phys.* B **17** 4585
[7] Jiang X C, Herricks T and Xia Y N 2002 *Nano Lett.* **2** 1333
[8] Balamurugan B, Mehta B R and Shivaprasad S M 2001 *Appl. Phys. Lett.* **79** 3176
[9] Geis M W, Efremow N N, Woodhouse J D, McAleese M D, Marchywka M, Socker D G and Hochedez J F 1991 *IEEE Electron Device Lett.* **12** 456
[10] Zhirnov V V, Wojak G J, and Choi W B, Cuomo J J and Hren J J 1997 *J. Vac. Sci. Technol.* A **15** 1733
[11] Kang D, Zhirnov V V, Sanwald R C, Hren J J and Cuomo J J 2001 *J. Vac. Sci. Technol.* B **19** 50
[12] Davis F 1991 *Proc. IEEE* **79** 702
[13] Nicolaescu I V, Tardos G, and Riman R E 1994 *J. Am. Ceram. Soc.* **77** 2265
[14] Sheppard L M 1990 *Am. Ceram. Soc. Bull.* **69** 1801
[15] Ponthieu E, Grange P and Delmon B 1991 *J. Eur. Ceram. Soc.* **8** 233
[16] Zhao Q, Xu J, Xu X Y, Wang Z and Yu D P 2004 *Appl. Phys. Lett.* **85** 5331
[17] Liu C, Hu Z, Wu Q, Wang X Z, Chen Y, Sang H, Zhu J M, Deng S Z and Xu N S 2004 *J. Am. Chem. Soc.* **127** 1318
[18] Tang Y B, Cong H T, Chen Z G and Cheng H M 2005 *Appl. Phys. Lett.* **86** 233104
[19] Shi S C, Chen C F, Chattopadhyay Surojit, Lan Z H, Chen K H and Chen L C 2005 *Adv. Func. Mater.* **15** 781
[20] Shi S C, Chattopadhyay Surojit, Chen C F, Chen K H and Chen L C 2006 *Chem. Phys. Lett.* **418** 152
[21] Wu Q, Hu Z, Wang X Z, Lu Y N, Huo K F, Deng S Z, Xu N S, Shen B, Zhang R and Chen Y 2003 *J. Mater. Chem.* **13** 2024
[22] Balasubramanian C, Godbole V P, Rohatgi V K, Das A K and Bhoraskar S V 2004 *Nanotechnology* **15** 370
[23] Wu Q, Hu Z, Wang X Z, Chen Y and Lu Y N 2003 *J. Phys. Chem.* B **107** 9726
[24] Yang H T, Shen C M, Su Y K, Yang T Z and Gao H J 2003 *Appl. Phys. Lett.* **82** 4729
[25] He S T, Yao J N, Jiang P, Shi D X, Zhang H X, Xie S S, Pang S J and Gao H J 2001 *Langmuir* **17** 1571
[26] Fan S S, Chapline M G, Franklin N R, Tombler T W, Cassell A M and Dai H J 1999 *Science* **283** 512
[27] Cao P J, Gu Y S, Liu H W, Shen F, Wang Y G, Zhang Q F, Wu J L and Gao H J 2003 *J. Mater. Res.* **18** 1686
[28] Liu F, Cao P J, Zhang H R, Tian J F, Xiao C W, Shen C M, Li J Q and Gao H J 2005 *J. Crystal Growth* **274** 126
[29] Liu F, Tian J F, Bao L H, Yang T Z, Shen C M, Lai X Y, Xiao Z M, Xie W G, Deng S Z, Chen J, She J C, Gao H J and Xu N S 2008 *Adv. Mater.* **20** 2609
[30] Fowler R H and Nordheim L W 1928 *Proc. R. Soc. London Ser.* A **119** 173
[31] Latham R V and Xu N S 1995 *High Voltage Vacuum Insulation* (London: Academic Press) P **127**
[32] Fursey G N and Vorontsov-Vel'yaminov P N 1968 *Sov. Phys: Tech. Phys.* **12** 1370
[33] Bonard J M, Weiss N, Kind H, Stöckli T, Forró L, Kern K and Châtelain A 2001 *Adv. Mater.* **13** 184
[34] Wang B P and Tong L S 1996 *Appl. Surf. Sci.* **94/95** 101